Theor Chim Acta (1988) 74: 403-414

Theoretica Chimica Acta

Dynamics of $H+O_2$ collisions on an *ab initio* potential energy surface

Ju Guan-zhi, Feng Da-cheng, Cai Zheng-ting and Deng Chong-hao

Institute for Theoretical Chemistry, Shandong University, Jinan, People's Republic of China

(Received November 20, 1987; revised and accepted March 3, 1988)

The dynamics of elementary rate processes for $H+O_2$ collisions on an ab initio potential energy surface have been simulated by quasiclassical trajectory theory (QCT). For $H+O_2$ ($v=0, j=1$), we have obtained the reaction probability P_r (E, b) as a function of collision energy E and impact parameter b, the reaction cross section S_r as a function of E, and the average values $\bar{v}'_\alpha$, $\bar{j}'_\alpha$ of the product quantum numbers of OH.

For $H+O_2$ ($v=2, j=1, 20, 40, 60, 80, 100$; $v=1, 3, 4, 5, j=1$) at $E=0.3$ eV, we have found that b_{max} is about $4.5a_0$ and the impact parameter at which P_r is maximum decreases as j increases. The reaction cross section increases as j and v become large. For inelastic collisions, when b is small and j is large, the $\bar{v}'_{O_2}$ and $\bar{j}'_{O_2}$ are both small. For reactive collisions, $\bar{v}'_{OH}$ almost equals zero, but the probability of $\bar{v}'_{OH}$ being larger than zero increases with increasing j; and v'_{OH} even shows population inversion for $j=100$. Additional details of the dynamics are shown in figures of interparticle distance and stereographs.

Key words: Quasiclassical trajectory calculation — $H+O_2$ — State distribution — Stereograph of collision trajectory

1. Introduction

Many experiments [1-3], and theoretical calculations [4-13] have been performed for the elementary reaction $H(^2S)+O_2(^3\Sigma_g^-) \rightarrow OH(^2\pi)+O(^3P)$. Schott [1] has measured its rate constant, Benson [4] has calculated the rate constant using simplified transition state theory (TST), Gauss [6] has given a modified London-Eyring-Polanyi-Sato-type (LEPS) potential energy surface (PES) and calculated

the rate constant for it, Redmon [7] has computed some reaction cross sections for selected states of the molecule O_2 with Gauss's PES using quantum scattering theory, and Miller [9] has calculated the rate constant on the Melius surface [8] by quasiclassical trajectories (QCT). In 1984, Woffrum's group measured some reaction cross sections [3]. Other studies include that of Kleinermanas and Schinke [11] who have reported the dynamics for the reaction at high collision energies, and our calculations of the A-factor on an *ab initio* PES using Eyring's TST [13]. We have also done some QCT calculations [12] and found that translational energy is almost unable to promote the reaction, but vibrational energy promotes the reaction well. This is similar to the result found by Bottomley et al. [10] on the Murrell semiempirical PES.

In this paper, the dynamics of $H+O_2$ collisions on Melius-Blint [8] PES have been simulated by QCT.

2. Potential energy surface and computation procedure

For the reaction system $H+O_2$, there are semiempirical PESs by Gauss [6] and by Farantos et al. [5], and an ab initio one by Melius and Blint [8]; the last one was employed for the QCT calculation presented here. The parameters of the PES are listed elsewhere [8].

The details of the calculational method have been described elsewhere [14–17]. Initial parameters, which were ramdomly selected for a set of trajectories were the impact parameter b, the vibrational phase, and the three orientation angles of the O_2 reagent molecule, while the parameters which were fixed for each set of calculations were the initial separation ρ between atom H and molecule O_2 ($10a_0$ in all the calculations reported here), the relative translational energy E, and the vibrational and rotational quantum numbers v and j of the reactant molecule. The final state properties which were obtained for each trajectory were the identity of the molecular product, the translational and internal energies, and the vibrational and rotational quantum number v' and j' of the product molecule. The continuous values of the classical vibrational and rotational quantum numbers were rounded off to the nearest integers.

The accuracy of the integration procedure used in the trajectory calculations was tested by back integration of some trajectories to reproduce the initial conditions and by checking conservation of total momentum and energy for each trajectory. The step size in the calculation reported here was 4.3×10^{-17} s, and at least 1000 trajectories were calculated for every set of v, j, and E.

3. Results and discussion

3.1. Reaction probability and cross section

The reaction cross section S_r (E, v, j) for a given set of initial conditions was calculated from the equation

$$S_r(\mathrm{E}, v, j) = 2\pi \int_0^{b_{\max}} P_r(\mathrm{E}, v, j, b) b \, \mathrm{d}b$$

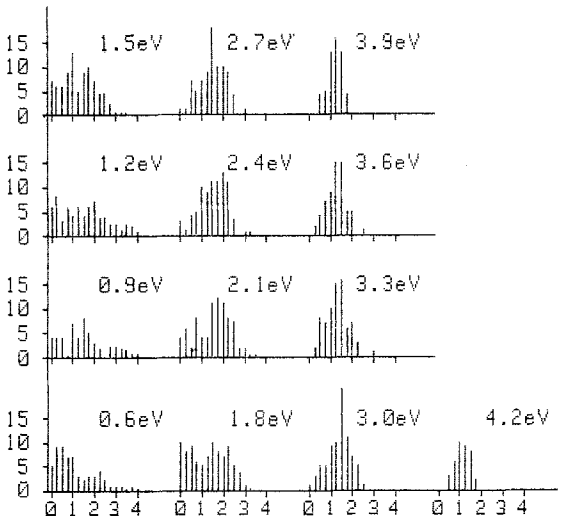

Fig. 1. Reaction probabilities $P_r(\%)$ as a function of impact parameter (a_0) at various relative translational energies for $v=0, j=1$

where b_{max} is the maximum impact parameter at which the reaction occurs, and $P_r(E, v, j, b)$ is the reaction probability as a function of impact parameter b for a fixed set of initial conditions (E, v, j).

For $H+O_2$ $(v=0, j=1)$, the reaction probabilities were computed at different relative translational energies and impact parameters and are shown in Fig. 1. From Fig. 1, it can be seen that the reaction probability varies slowly with the impact parameter b at low collision energies. Reaction can occur out to $4a_0$. When the relative translational energy E is increased, the range of b at which the reaction occurs decreases. The range shortens from both directions: (i) as E goes up from 0.6 to 4.2 eV, b_{max} decreases from $4.0a_0$ down to $2.0a_0$, and (ii) at small b, as E increases from 3.0 eV to 3.9 eV, the minimum b at which reaction occurs goes up from 0 to $0.25a_0$. However, in the range of middle b, as E increases P_r increases greatly. In other words, the selectivity of the reaction on b is enhanced when E increases. The cross section S_r as a function of collision energy E is

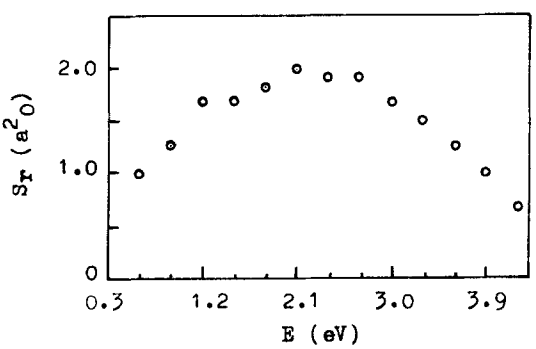

Fig. 2. Cross sections at various relative translational energies for $v=0, j=0$

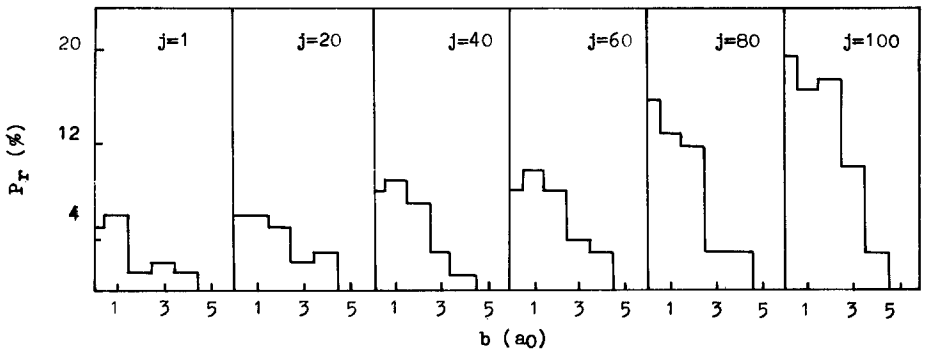

Fig. 3. Reaction probabilities as a function of impact parameter b at $v=2$, $E=0.3$ eV

plotted in Fig. 2, from which it can be seen that at $E=2.1$ eV, S_r (E) has a maximum equal to about $2a_0^2$.

P_r (E, v, j, b) for $H+O_2$ ($v=2, j=1, 20, 40, 60, 80, 100$) at $E=0.3$ eV is depicted in Fig. 3, and it can be seen that for the six rotation states of O_2, the reaction probability decreases substantially as b increases. For all j states, however, the maximum impact parameter is $4.5a_0$, i.e. $P_r=0$ for $b>4.5a_0$. The impact parameter at which the reaction probability is maximum is about $1a_0$ for $j=1$–60, but P_r peaks at the origin for $j=80$ and 100. In all cases P_r at fixed b becomes

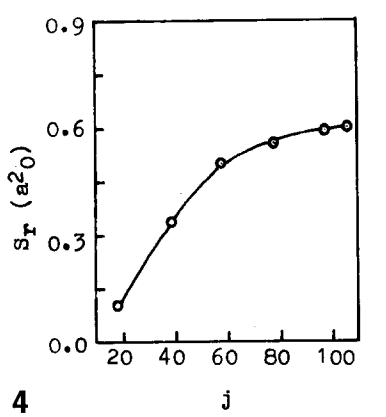

4

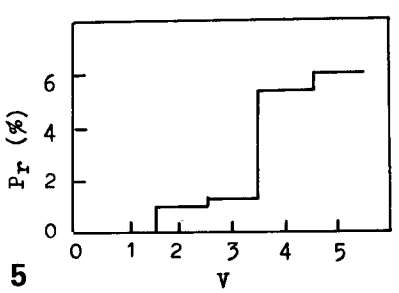

5

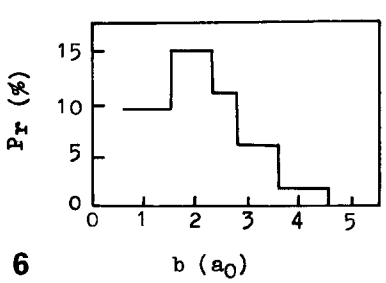

6

Fig. 4. Reaction cross sections as a function of j at $v=2$, $E=0.3$ eV

Fig. 5. Reaction probabilities as a function of v at $j=1$, $b=3a_0$, $E=0.3$ eV

Fig. 6. Reaction probabilities as a function of impact parameter b at $v=5$, $j=1$, $E=0.3$ eV

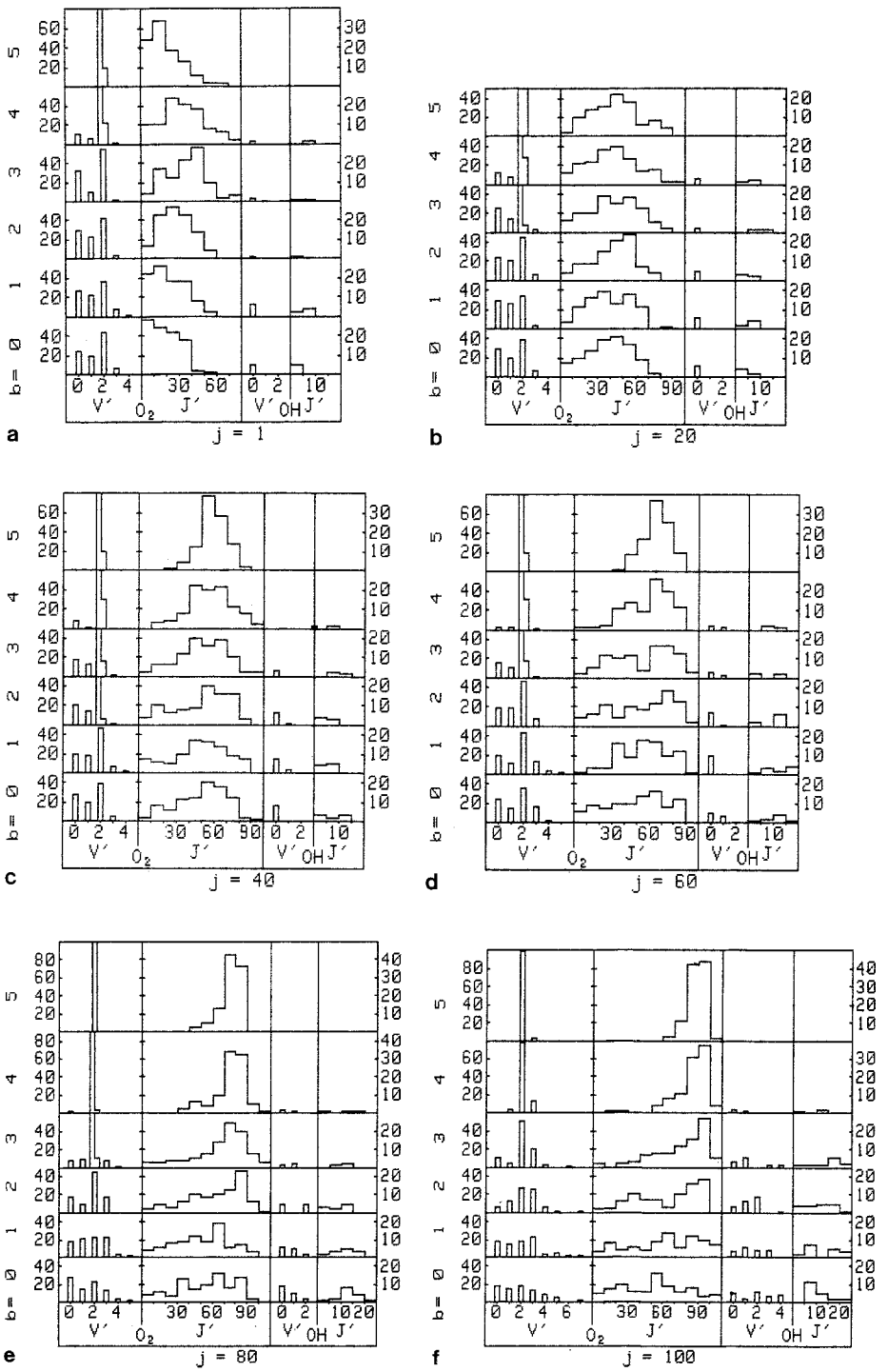

Fig. 7a–f. State distributions of products, P_i (v') and P_i (j') in %, at $v=2$, $E=0.3$ eV

larger with increasing j for $b \leq 3a_0$. Reaction cross sections $S_r(j)$ are plotted as a function of j in Fig. 4. As shown in Fig. 4, $S_r(j)$ increases monotonically as j increases, meaning that high rotational excitation favors the reaction; this result is similar to that found by Miller [9] and by Bottomleyet et al. [10]. The reaction probability for $E = 0.3$ eV, $j = 1$, and $b = 3a_0$ is displayed as a function of the vibration state v of O_2 in Fig. 5. It is apparent that, with the exception of $v = 0$ and 1 the reaction probability $P_r(v)$ increases with increasing v. The variation of P_r with b for high vibrational states (Fig. 6) is similar to that for $v = 2$ (Fig. 3).

3.2. Distribution of products

The probability of the product i being in the vibrational state v' and rotational state j' is defined as

$$P_i(v') = N_i(v')/N \tag{1}$$

$$P_i(j') = N_i(j')/N \tag{2}$$

where N is the total trajectory number, and $N_i(v')$ and $N_i(j')$ are the number of trajectories leading to product i in the vibrational state v' and rotational state j' respectively. As shown in Fig. 7 (a)-(f) for reagent molecule O_2 with $v = 2$ and $j = 1, 20, 40, 60, 80, 100$, when b is large ($4a_0$ and $5a_0$) the collision is essentially elastic and the vibration state of molecule O_2 (collision product) does not change readily; furthermore, the probability for $j' < j$ is almost equal to that for $j' > j$ (except $j = 1$). The probability of finding O_2 with vibrational state $v' < 2$ goes up as b goes down; for example, when $b = 1a_0$ and $j = 20$ the probability that the product O_2 has vibration quantum number $v' = 0, 1, 2$ is almost the same, and the probability of finding O_2 with rotational state $j' < j$ becomes very large. When b decreases the probability of the product O_2 having vibrational state $v' > 2$ increases; for example, at $b = 0$ and $j = 100$ the probability for $v' = 3, 4, 5$ is very large.

In brief, the smaller the impact parameter b and the larger the excited rotational state j of reagent molecule O_2, the larger the probability that the O_2 will have vibrational quantum number $v' \neq 2$ and rotational quantum number $j' < j$. These results show that for small b the collisions show considerable vibrational and rotational inelasticity, and the inelasticity increases as b decreases.

For reactive collisions, when $j < 40$ and $0 < b < 4a_0$ the product OH is mainly in the ground state. With increasing rotational quantum number j for the reagent molecule O_2, the probability of producing OH with $v' > 0$ increases; for example, for $b \leq 2a_0$ and $j = 100$, some inversion of the populations for the vibrational states of OH appears. These results are similar to those found previously [11] for a collision energy equal to 3.9 eV.

Table 1. The average collision time at various collision energies

E (eV)	Average collision time (s)[a]	cpu time(s)[b]
0.6	2.4×10^{-13}	7.4
1.5	9.2×10^{-14}	2.8
2.4	6.5×10^{-14}	2.0
3.9	3.9×10^{-14}	1.2

[a] Defined as the time when the reagents are separated by $10a_0$ or less
[b] The computer is FACOM M340 (Shandong University)

Table 2. Percentage of backward scattering ($\theta > 90°$) trajectories for the reactive process

E (eV)	OH scattered backwards (%)
0.0–2.1	59
2.4	59
2.7–4.2	60

3.3. The mechanism of collision

As discussed previously [12], the trajectories of the reaction $H+O_2$ are generally complicated. After oscillating many times in the potential well, the complex can dissociate. With increasing collision energy, this occurs more easily, and the lifetime of the complex decreases (Table 1).

Figure 8 shows two reactive collisions with the same initial position vector and impact parameter but different collision energies, and it shows how the distance

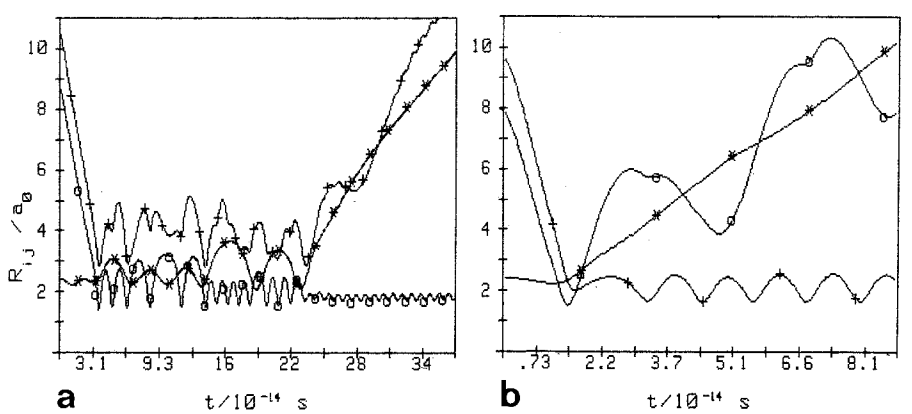

Fig. 8a, b. Two reactive collision trajectories with the same initial position vector and the same impact parameter b, but different relative translational energies: **a** E = 0.6 eV; **b** E = 4.2 eV. * OO; ○: OH; +: OH

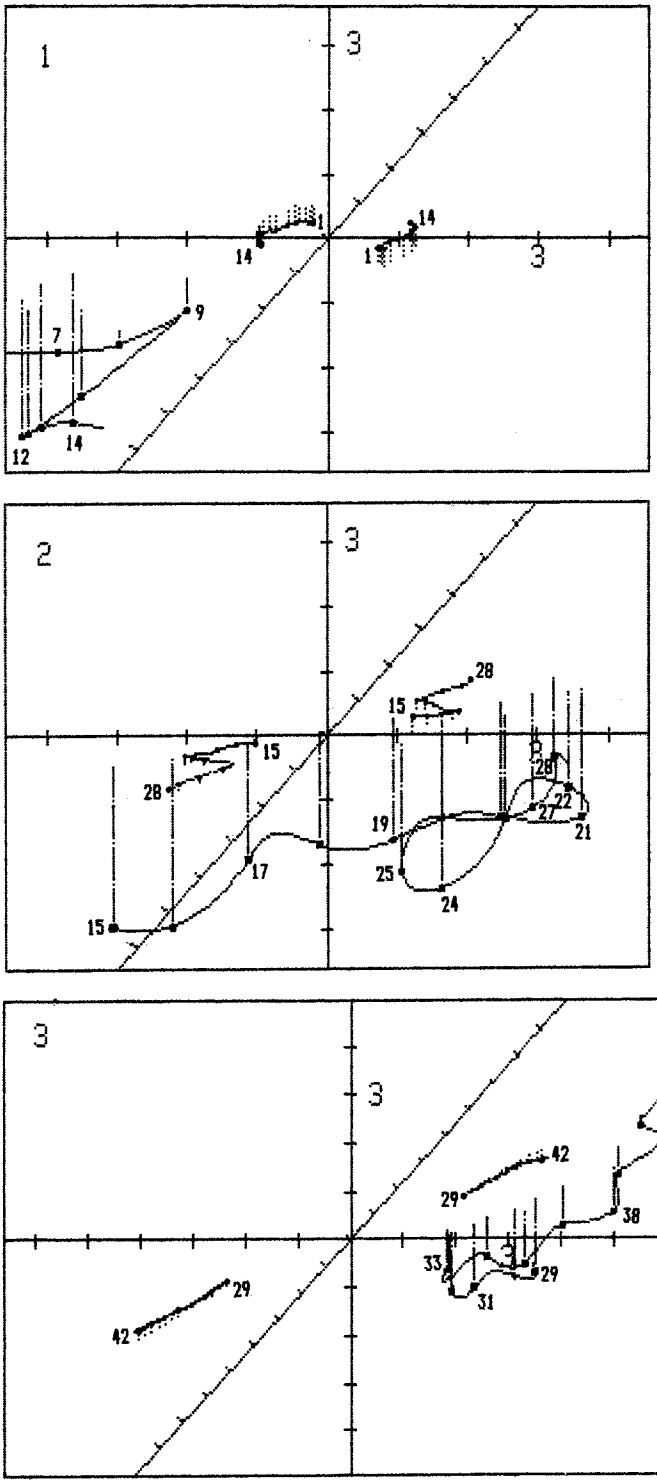
1
3
14
14
1
3
9
7
12
14
2
3
28
15
15
28
15
17
19
25
24
28
22
27
21
3
3
42
42
29
38
33
3
29
31
6
29
42

a

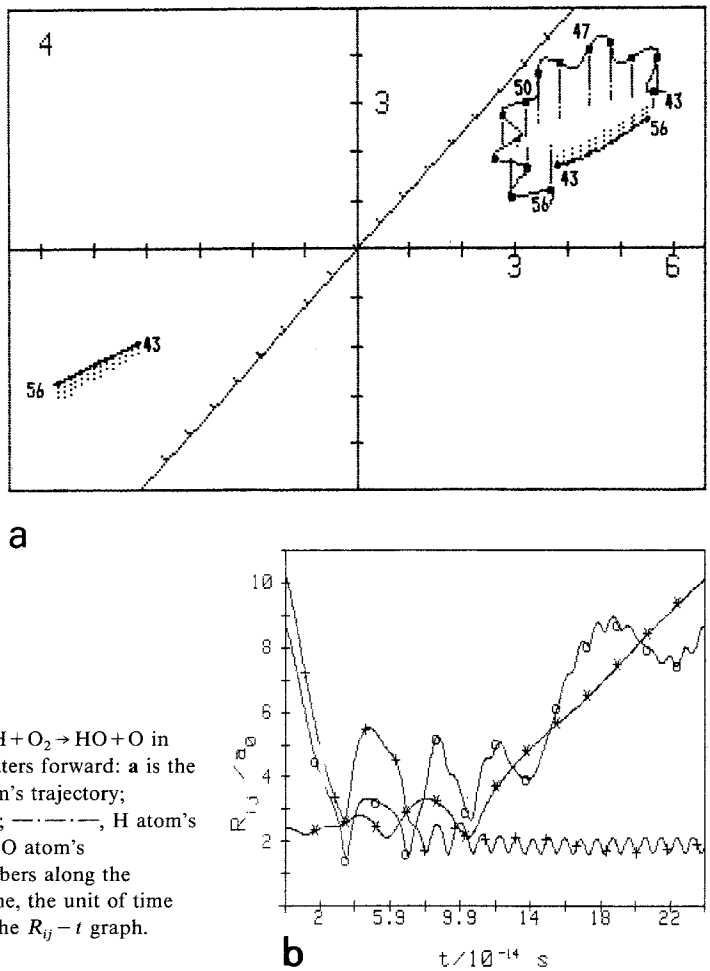

Fig. 9a, b. A reaction $H+O_2 \rightarrow HO+O$ in which the product scatters forward: **a** is the stereograph. ■, H atom's trajectory; ●, O atom's trajectory; —·—·—, H atom's z-coordinate; – – – – –, O atom's z-coordinate. The numbers along the trajectory represent time, the unit of time being 5.96E-15 s. **b** is the $R_{ij}-t$ graph. Symbols as in Fig. 8

between each pair of atoms varies with time. A trajectory at collision energy 0.6 eV is shown in Fig. 8a, and one at 3.9 eV in Fig. 8b; the latter is much simpler than the former. In order to visualize the collision dynamics more clearly, stereographs [19] of the collision trajectories have been plotted in Figs. 9–10, from the mechanism, and especially the movement of the system in space, is more easily understood. It is difficult to get good statistics for the distribution of the scattering angles of the product OH because the probabilities of reactive collisions are small. The distribution of scattering angles of product OH at E = 2.4 eV is shown in Fig. 11, where the total number of trajectories is 8050, and the number of the reactive trajectories is 569.

From Fig. 11, we can see that there are two maxima in the distributions, one at the scattering angle $\theta = 10°$–$40°$ and the other at $\theta = 140°$–$170°$, and the probability of sideways scattering is very small. The ratio of the number of backward scattering reactive trajectories to the total number of reactive trajectories is very close to

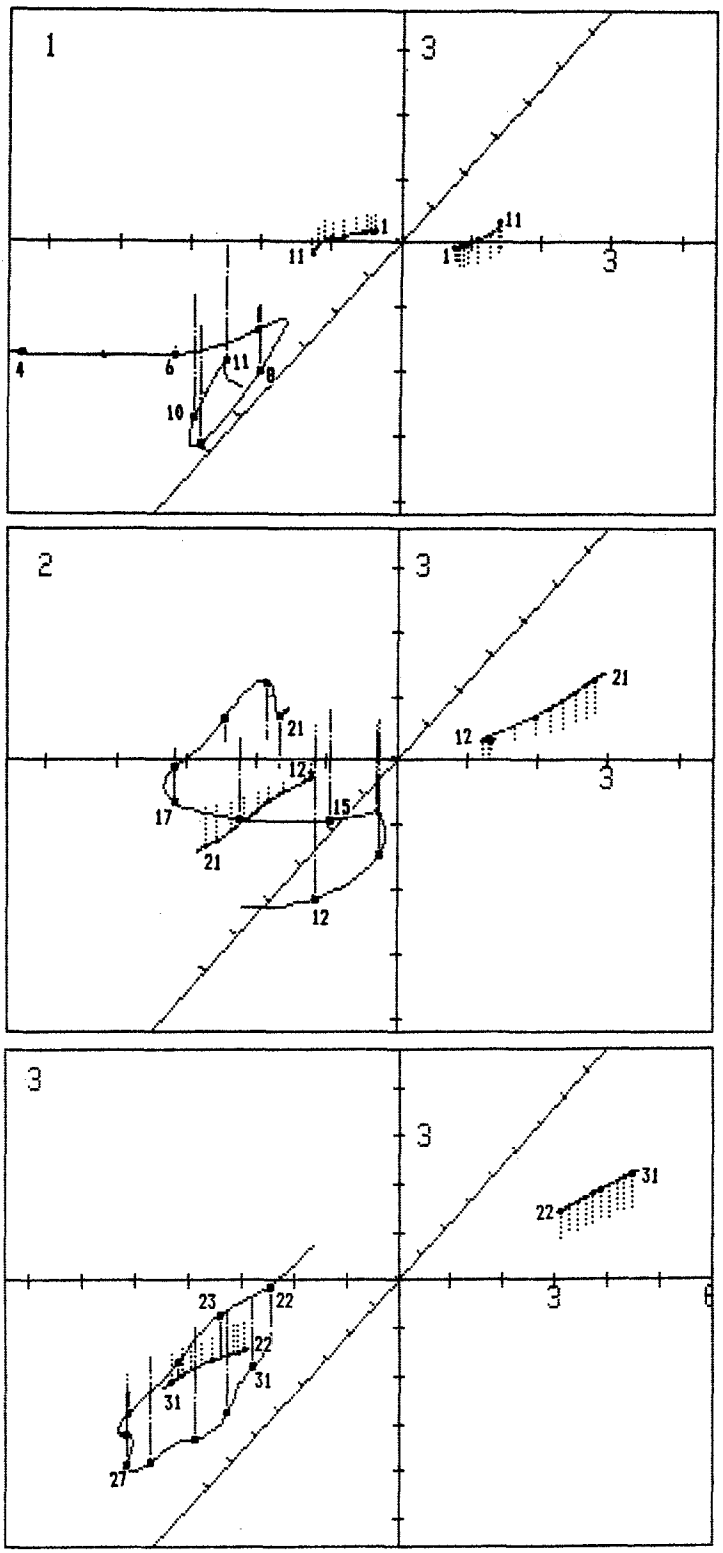
1
3
11
1
1
11
3
4
6
11
8
10
2
3
21
12
3
17
15
21
12
3
3
3
22
31
3
23
22
22
31
31
27

a

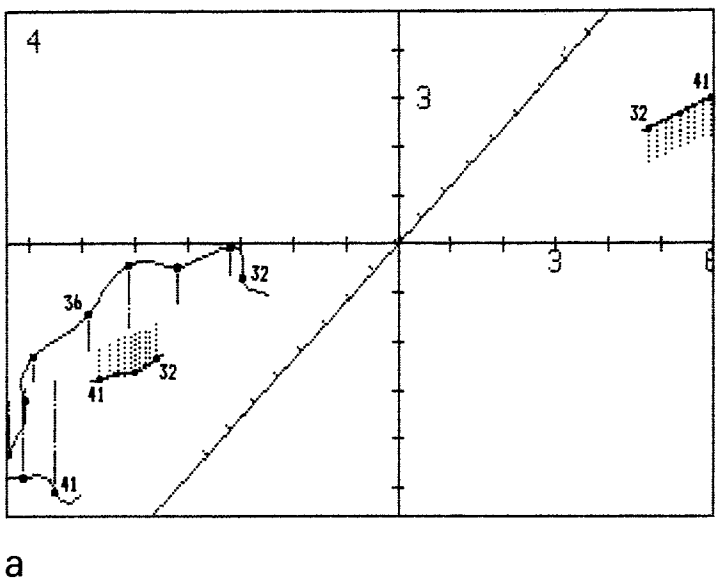

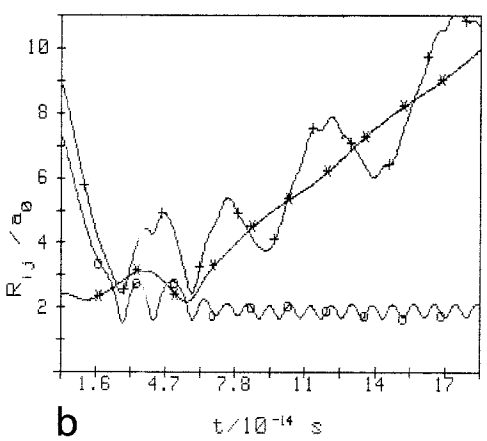

Fig. 10a, b. A reaction $H+O_2 \rightarrow HO+O$ in which the product scatters backward. The labelling is the same as in Fig. 9, but the unit of time in **a** is 3.93E-15 s. Symbols as in Fig. 8

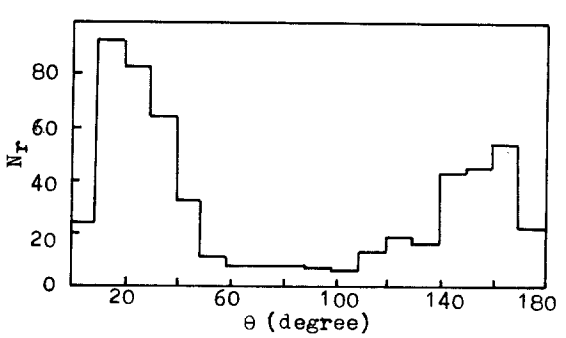

Fig. 11. Distributions of scattering angles of the product OH

50% at all collision energies (Table 2). This indicates [18] that the reaction of $H+O_2$ proceeds through a long-lived complex.

Acknowledgment. The authors are pleased to thank Professor Donald G. Truhlar and Professor Joel M. Bowman for their useful discussions and help.

References

1. Schott GL (1973) Combust Flame 21:357
2. Baulch PL, Drysdale DD, Horne DG (1973) 15th Symposium (international) on Combustion. The Combustion Institute, Pittsburgh
3. Kleinermanns K, Wolfrum J (1984) J Chem Phys 80:1446
4. Benson SW, Golden DM, Lawrence RW, Shaw R, Woolfolk RW (1975) Int J Chem Kinet Symp 1:399
5. Farantos S, Leïsegang EC, Murrell JN, Sorbie K, Texeira-Dias JJC, Varandas AJ (1977) Mol Phys 34:947
6. Gauss JrA (1978) J Chem Phys 68:1689
7. Redmon MJ (1979) Int J Quant Chem Symp 13:559
8. Melius CF, Blint RJ (1979) Chem Phys Lett 64:183
9. Miller JA (1981) J Chem Phys 74:5120
10. Bottomley M, Bradley JN, Gilbert JR (1981) Int J Chem Kinet 13:955
11. Kleinermanns K, Schinke R (1984) J Chem Phys 80:1440
12. Ju G (1985) J Mol Sci 3:159
13. Ju G, Feng D, Deng C (1985) Acta Chimica Sinica 43:680
14. Karplus M, Porter RN, Sharma RD (1965) J Chem Phys 43:3295
15. Porter RN, Raff LM (1976) Classical trajectory methods in molecular collision, In: Miller WH (ed) Dynamics of molecular collision, part B, vol 2. Plenum Press, New York, p 1
16. Kuntz PJ (1976) Features of potential energy surface and their effect on collision, In: Miller WH (ed) Dynamics of molecular collisions, part B, vol 2. Plenum Press, New York, p 55
17. Truhlar DG, Muckerman JT (1979) Reactive scattering cross sections. In: Bernstain RB (ed) Atom-molecule collision theory. Plenum Press, New York, p 505
18. Wolfgang R (1976) Discussions Faraday Soc 44:80
19. Feng D, Ju G (1987) J Mol Sci 5:201